Research Article

Design and execution of Quadratic Boost Converter (QBC) in Renewabe Energy Synergies

Angalaeswari S., Deepa.T*, Subbulekshmi.D, Krithiga S., Pramit Ghosh, Aniket Kumar, Mutthi Karunanidhi

School of Electrical Engineering, Vellore Institute of Technology, Chennai.

Article History: Received: 10 January 2021; Revised: 12 February 2021; Accepted: 27 March 2021; Published Online: 20 April 2021

ABSTRACT: The Output Voltage Of The Renewable Energy Sources Such As Solar Is Very Low Which Is Not Sufficient To Drive The Loads In Practical. To Increase The Voltage Level, There Are Various Boost Converter Configurations Available In The Literature. The Significant Structure Is The Quadratic Boost Converter Which Has So Many Advantages Than The Conventional Converters. In This Paper, Novel Quadratic Boost Converter Is Proposed And Implemented In Hardware Prototype And The Experimental Results Are Compared With The Designed Values. The Results Show That The Proposed Converter Is Having Similar Results In Both Calculated And Real Time Values With Higher Efficiency.

KEYWORDS: Quadratic Boost Converter, Solar System, Enhanced Efficiency, Hardware Prototype.

1. Introduction

A conventional Boost Converter (BC) has multiple switching characteristics which increasing the I^2R losses and therefore, is not fit for implementation in the high-power industries where usage of high efficiency is point of everything. Therefore, a Quadratic Boost Converter (QBC) is proposed which is the cascaded form of two conventional boost converters wherein one switch is functioning in the form of a MOSFET which reduces losses and therefore increases efficiency. The cons are low saturation points and unstable voltage control.

Authors [1] explained the necessity of the present era to diminish the non-conventional sources from the livelihoods. The difference in oil-based vehicles and electrical vehicles with hybrid electric vehicles has been discussed. Ongoing progressions in DC-DC converters proved to be proper for electric vehicles. There is a need for many DC supplies to charge battery operated vehicles.

Single energy unit voltage yield is generally 1.5V. To build the voltage power devices masterminded in a stacked way, the voltage is then taken care by the BC. Added, the boosted voltage is taken care of through an inverter to accomplish the wanted air conditioning voltage and recurrence for utility matrix [2].

In these applications, the ratio of the output and input voltage also known as the gain required to be fairly increased. Still, conventional BCs may be used to implement such a high gain owing to the constraints like a very small off-time for the converter switches, the high-voltage stress on the switches, and less efficiency [3]. Conventional BC operates at increased saturation period for advanced addition [4]. At high obligation cycle, inductor will become saturated, whereas QBC works at low saturation cycle.

The cascaded BC configuration is constructed using conventional BCs in two or more blocks in series for increasing the voltage at the output level. Even though, adding the number of BCs in cascaded mode can reduce the stress in current of lower phases and stresses in voltage of higher stages, but it rises the losses in the circuit [5].

The diodes conducts softly and the inverse-recovery problems are greatly lightened [6]. Also working at stable frequency and with less commutation losses, the stress on the voltage and current in the proposed converter are comparable to the conventional “hard-switched” corresponding item.

The parts' voltage appraisals and energy capacities of latent segments of the proposed one are enormously decreased contrasted with the regular zero-voltage-progress converter. Voltage change proportion is nearly multiplied contrasted with the customary lift converter. Augmentation of the projected idea to acknowledge polyphase DC-DC converters is discussed [7].

The principle R2P2 is helpful for growing new converters. These have wide transformation proportions and quadratic reliance regarding the obligation proportion. In this investigation, the voltage transformation proportions, normal models and consistent state working conditions for proposed converters are determined, which are confirmed by test results [8].

During switch off period, two capacitors are equally charged and the energy is released to meet high voltage gain during the switch-on period coupled inductor. Furthermore, the leakage energy of the coupled inductor is reused with an uninvolved brace circuit. In this manner, the voltage stress on the fundamental switch is diminished. The switch with less opposition drain source on resistance also called as RDS (ON) can be received to reduce the loss in the conduction mode [9].

Renewable and sustainability are the two amenities that world focuses on commencing any technology to the society [10]. Solar energy extraction and producing electricity and power generation are vowing in various applications. The solar panels and PV system technologies include design of PV cells, design of converter topologies and its control strategies. The PV output depends on voltage, current and power that varies with atmospheric conditions. A DC-DC converter is needed to get a high voltage. The high step up and conversion ratio is achieved with quadratic boost converter (QBC) with low duty cycle. The switching operating conditions of the converter are considered and expressed as quadratic equations, and the expression for conversion ratio is obtained. The control algorithm is proposed for the converter to achieve high performance irrespective changes of the PV parameters. The fuzzy logic with MPPT tracking algorithm seems to be highly efficient for changing operating conditions and testing of dynamic performance. The input parameters to the controller are considered as voltage and power and the duty cycle is given as output that controls the switch of the converter.

The quadratic boost converters are improved with the changes in topologies of the circuit and control algorithm. An improved topology with two QBC interleaved and phase shifted is proposed to reduce the current ripple and provide voltage lift through the capacitor. The capacitor is connected intermediate to the two QBC converters along with the intermediate diode which prevents the capacitor from discharging. Provision of control algorithms and artificial network tools are not used to get a high step-up ratio, a simple closed loop is proposed. The advantages of the converter include compact size, low current ripple, improved conversion ratio and increased efficiency. The conversion ratio is obtained by voltage- second and Kirchhoff's voltage law (KVL) principles[11].

L. Xie et al designed the energy storage elements in converters are crucial for getting a better performance. The order of the elements is not integer based instead the capacitors and inductors are fractional order. The equivalent circuit and parameter modelling of the circuit with fractional order elements are on the basis of Caputo and R-L definitions. The analysis of the fractional order values of the storage elements has better current and voltage responses which embellishes the performance of the converter. R-L definition for deriving fractional orders and implementing in the circuit of converter model is the optimal design approach for DC-DC converters.

The converter topology is constructed with cascade connection of buck-boost and boost converters [13]. The topology has high conversion gain with ripple free current and at optimal range of duty cycle. The duty cycle is varied a selectable range. The components of the elements are reduced related to conventional converter topologies in the literature.

The quadratic converter with tapped inductors is replaced with coupled inductors. When the output voltage is high, the coupled elements having same turns ratio discharge at the equal time [14]. The voltage stress of the capacitor decreases at lesser duty cycle. The stress on the voltage level of the switches is decreased by the topology change with secondary coupled inductors placed in the output side.

The conversion ratio of conventional BC rests on the duty cycle whereas in QBC, the conversion ratio is square of duty cycle. The switching frequency is a function of duty cycle and by providing phase shit control for the switching technique increase the frequency values of voltage and current ripples. The design of coupled inductors should be considered with its coupling coefficient (k) parameter. The k value influences the performances of the interleaved converters with coupled inductors wound on the magnetic core. The k values are design based on the direction of windings of the inductors. The optimal value of coupling coefficient is to maintained to achieve higher conversion ratio. Tight coupling with $k = 0.8$ approximately with duty ratio 0.5 to the switch is applied to quadratic converters [15].

The selection of rules and membership function for the fuzzy logic is determined by the trial-and-error method which degrades the performance of the system. The uncertainties in the solar system are based on the atmospheric surroundings. The inputs to the controller are considered as change in voltage and change in power. To handle this uncertainty in PV system a new type of fuzzy logic is proposed [16]. Two type of fuzzy sets are used here the first set is a blurred triangle with its membership function the second set is the extension of type 1 fuzzy set. Type -2 set is a robust structure and it has a high rejection capability against various uncertainties.

A single switch combining traditional buck and boost inverter operation is proposed. The topology is simple structure, the stress and current ripples are reduced. It can operate with wide conversion ratio with low duty cycle. A unique feature of this is by adding the inductor element in the input and output ports which reflects in the current drawn in the circuit. The input port and output current are continuous [17].

The two boost converters topologies are cascaded to activate a single switch. The gating signal to activate the switch is provided by hard switching signal from PWM techniques. The PWM technique is interfaced with MPPT algorithm provided with variable duty cycle [18]. The PV system uncertainties with respect to solar irradiation levels and climatic conditions are considered in the MPPT algorithm.

The MPPT algorithm is the most common tracking algorithm used in renewable power generation applications. Radial based neural network is proposed for wind energy system with the parameter input taken as wind velocity. The DC conversion process for the renewable energy sources is proposed with a boost converter and a SEPIC converter and compared its performance with quadratic boost converter. The maximum power is extracted from the wind speed. The duty cycle of the switch of BC is obtained by the DC link voltage tracking the maximum power [19]. The duty cycle at the output neuron is determined based on the input neurons of the generated voltage and current. The error in each layer of the neural network is given feedback to the controller and adjusted according to the desired wind speed. The major advantage of radial basis neural network with QBC converter has less settling time than other controllers which can be realized in practical manner.

Transformer less semi converter operation of QBC has advantages with increased and reduced voltage ratio conversion properties. The stress on the voltage level of the switch is low, with low current ripple. The projected converter operates with two switches, one in the input port side and other in the output port side. One operation is used for step up and other for step down. The voltage conversion ratio and the relation of the duty cycle varies exponentially, hence the conversion ratio is in ultra-range [20].

The advantage of coupled inductors in QBC is it has high voltage gain rather than using inductor in the topology. High gain is achieved by the turns ratio windings of the coupled inductors. The stress of the switch may increase due the effect of leakage inductance from the coupled inductor. When the magnetic flux of one inductor in mutual inductance does not share the flux with the second inductor leakage inductance occurs. A passive clamping circuit is added to the QBC to compensate for the leakage inductance and to reduce the high voltage stress [21].

The voltage gain of the converter with tapped inductor is low, which can be solved by integrating it with step up capabilities of QBC. The structure reduces the stress of the active switches and the current drawn in the circuit is ripple free and continuous. The advantages of semi tapped and full tapped QBC is proposed here like in the use of micro-inverter in non-conventional energy applications. The efficiency of the full tapped converter is high than in semi tapped QBC.

The projected converters are considered from quadratic lift converter structure having same number of components of the QBC and comparable quadratic change proportion. The voltage drops of semi tapped is high compared to full tapped topology. Fully tapped inductor has to be designed with less turn ratio as the pulsating input current i9ncreases with increase in coupling coefficient and turn ratio. Tapped-inductor topology are designed for high voltage gain based on turn ratio and duty ratio of the inductor. The proposed converter has small voltage rating design of components and low on-state resistance of the active switch [22].

The quadratic boost converter is proposed with voltage multiplier cells which can reduce the effect of stress in the semiconductor switches of the converter [23]. Addition of switch or inductors or components in the converter are not required. The cells in the voltage multiplier play the major role to boost the voltage gain, reducing the switch stress and to minimize the losses. The topology is similar to voltage lifting capacitor or any voltage lifting technique topologies. The size of the inductor is heavy compared to the other converters. This converter operates similar to single active switch, and will operate using the control circuit with simple structure of the converter.

For high step up voltage new topologies and cascade converters are proposed which increase the number of components and the weight of the structure. To get high step up voltage a CLD cell is added to the QBC topology. The topology consists of energy storage elements capacitors, inductor and diode which help in stepping up the voltage of the converter at the output level. A single switch is incorporated and the stress of the switch voltage level is low by the introduction of CLD cell in the circuit. The waveform of the current and voltage time period is done for one switching cycle and the switching frequency is higher than the fundamental frequency. The AC ripple in the voltage and current waveform is less. CLD cell have better characteristics regarding the high voltage step-up ratio, decreased switch and diodes voltage stress [24].

The increasing demand on fossil fuels and power generation and distributed attracted the renewable energy sources [25]. The common Renewable source used widely is the photovoltaic system. The solar energy is the available energy and the extraction of power from them is captured by the cells and modules designed. To ensure peak power from the solar system the MPPT algorithm is incorporated along with the PV system. For connecting to the utility grid, the atmospheric conditions and the external components or sources connected in the neutral bus of the power system network which is considered in the algorithm.

The PV cell performance depends on the following parameters such as open circuit voltage (Voc), short circuit current (Isc), peak power point voltage (VMP) and peak power point current (IMP). The parameters are tested under the operating conditions of the practical system tied with the grid system. At short circuit and open circuit conditions, the V-I characteristics of the cell is observed. The MPPT algorithm use this characteristic and track the maximum power point with input parameters open circuit voltage and change in power in the PV module/cell circuits.

The temperature level of the solar cell increases owing to the rise in solar intensity and because of the energy loss in PV system. The output of PV system is inversely proportional to the temperature. The MPPT algorithm uses various methods to achieve the maximum power. The methods such as Perturb and Observe (P&O) method, Hill Climbing (HC) and Incremental conductance are deployed in autonomous and grid connected systems. The MPPT algorithm is done in Off-Line mode with solar PV modelling based on the datasheet parameters and V-I curves. The parameters are used in mathematical experimental formulas for getting the control signals of PV system, which are included in the operation of MPPT.

The cell voltage of the PV is very less which cannot be used to for interacting in grid tied systems. Hence, BC are included to boost up the voltage of the PV cell. The DC-DC converters include manty topologies in the literature. The conventional converters are tested with transformer and boosting the voltage to attain the increased voltage and high conversion ratio. A remote converter gives the separation between both the side circuits that is more useful in the design of the multiple output ports having different voltage levels. The basic DC-DC converters available are buck, boost, Cuk, SEPIC.

The constant research in the area of material and power electronics technology has enhanced the performance of the DC-DC converters which help to improve the system and applications interfaced with them.

The concept of changing the energy storage elements and switching cycle of switch in QBC will not ensure the control of instantaneous over current and over voltage. The average current mode control is applied to the converter to control the overvoltage and current to improve its power quality. The compensator networks are added to the QBC and voltage transfer ratio and current- voltage gain of the input and output port is evaluated and the characteristics curves are plotted. The PWM generator uses the signal of the compensator circuits for voltage and current as reference value and compute the closed loop control. The power loss in the circuit is reduced and the efficiency of the system is improved. Th input filter design for the converter is made simple as the overcurrent and overvoltage drawbacks are reduced by the average current control method.

2 Mathematical Modelling

2.1. DC-DC Converter

The relationship between voltage-current in an inductor is given as: $V = L\frac{di}{dt}$ (1)

MODE 1 (When the SWITCH is ON)

$$\Delta i = \frac{(V_{in} - V_t)T_{on}}{L} \quad (2)$$

MODE 2 (When the SWITCH is OFF)

$$\Delta i = \frac{V_{out} - V_{in} + V_d)T_{off}}{L} \quad (3)$$

By equating Δi:

$$V_{out} = \frac{V_{in} - V_t D}{1 - D} - V_D \quad (4)$$

In equation 4, the voltage drop across diode V_D and transistor V_T are neglected and written as in equation 5,

$$V_{out} = \frac{V_{in}}{1-D} \quad (5)$$

$$\frac{V_{out}}{V_{in}} = \frac{1}{1-D} \quad (6)$$

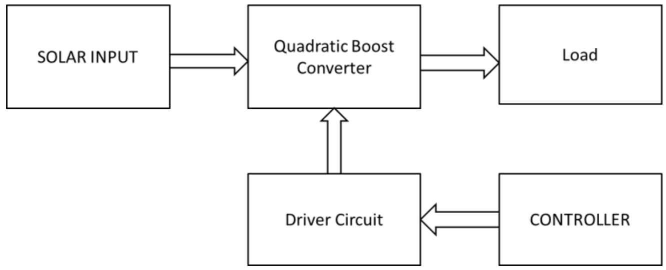

Fig 1. *Block diagram of proposed QBC*

The structure of the QBC and its operation is given in Fig.1. The input voltage is acquired through a solar panel which acts as variable voltage source. It is fed to the converter in which, the output voltage is supposed to be 4 times the voltage at input level. The BC increases the input voltage to higher voltage as the output. The resistance acts as a load to the circuit. The controller circuit is required to control the variable voltage and yield a constant voltage during closed loop operation.

2.2. Quadratic Boost Converter

Mode 1 (Switch on)

The assumption made in the analysis are i) the switch is in ideal condition, ii) capacitors C_1 and C_2 is considered to have large value in order to have constant voltage across the capacitors V_{C1} and V_{C2} during switching period. At the instant of switch on of S, D_3 is forward biased, and D_1, D_2 are reverse biased. The current in inductors L_1 and L_2 which are supplied by the input voltage V_{in} and C_1 respectively.

$-V_{in} + V_{L1on} = 0; \quad V_{in} = V_{L1on}$ (7)

$-V_{C1} + V_{L2on} = 0; V_{L2on} = V_{C1}$ (8)

Mode 2 (Switch off)

In this mode, both D_1 and D_2 are forward biased, and D_3 is getting reverse biased. Currents through L_1 and L_2 are used to charge C_1 and C_2 respectively with reduced value of i_{L1} and i_{L2}.

$V_{C2} = V_{out}$ (9)

$-V_{in} + V_{L1off} + V_{C1} = 0$ (10)

$-V_{C1} + V_{L2off} + V_{C2} = 0$ (11)

Applying Volt-Sec Balance:

$DV_{L1on} + (1-D)\, V_{L1off} = 0$ (12)

$DV_{in} + (1-D) * (V_{in} - V_{C1}) = 0$ (13)

$DV_{C1} + (1-D) * (V_{C1} - V_{C2}) = 0$ (14)

From (13),

$DV_{in} + V_{in} - DV_{in} - V_{C1} + DV_{C1} = 0$ (15)

$V_{in} - (1-D)\, V_{C1} = 0$ (16)

$V_{C1} = \frac{V_{in}}{1-D}$ (17)

From (14),

$D\frac{V_{in}}{1-D} + (1-D) * (\frac{V_{in}}{1-D} - V_{out}) = 0$ (18)

$DV_{in} + (1-D)^2\, V_{out} = 0$ (19)

$\frac{V_{out}}{V_{in}} = \frac{1}{(1-D)^2}$ (20)

2.3. Load calculations

Power(P) = Potential difference (V) * Current (I); According to the ohm's law ,I = $\frac{V}{R}$
Using the relation among the voltage, current, resistance and power the load value is determined as:

$$\mathbf{R} = \frac{V^2}{P} \tag{21}$$

3. Design Approach

The components present in BC are inductors, capacitors and semiconductor gadgets such as diodes, MOSFET, IGBT. A suitable selection of parts for demonstrating is depicted in Fig.2.

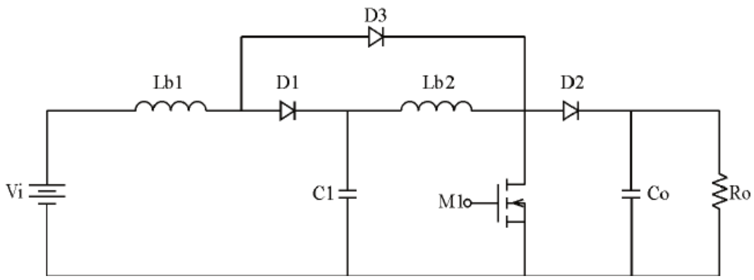

Fig.2 *Circuit diagram for the mathematical modelling*

During ON condition of the switch, the state variables are represented in differential form as follows:

$$\Delta i_{L1}=\frac{\mathrm{Vin}}{\mathrm{L1}} \ \& \ \Delta i_{L2}=\frac{\mathrm{Vc1}}{\mathrm{L2}} \tag{22}$$

$$\Delta \mathrm{V}_{C1}=-\frac{\mathrm{iL2}}{\mathrm{C1}} \ \& \ \Delta \mathrm{V}_{C2}=-\frac{\mathrm{Vout}}{\mathrm{Rc2}} \tag{23}$$

Similar way, the equation for the OFF condition is

$$\Delta iL_1=\frac{\mathrm{Vin}}{\mathrm{L1}}-\frac{\mathrm{Vc1}}{\mathrm{L1}} \ \& \ \Delta iL_2=\frac{\mathrm{Vc1}}{\mathrm{L2}}-\frac{\mathrm{Vout}}{\mathrm{L2}} \tag{24}$$

$$\Delta \mathrm{V}_{c1}=\frac{\mathrm{IL1}}{\mathrm{C1}}-\frac{\mathrm{IL2}}{\mathrm{C1}} \ \& \ \Delta \mathrm{V}_{out}=\frac{\mathrm{IL2}}{\mathrm{C2}}-\frac{\mathrm{Vout}}{\mathrm{Rc2}} \tag{25}$$

Average Model Equation of QBC:

$$\Delta iL_1=\frac{\mathrm{Vin}}{\mathrm{L1}}-\frac{\mathrm{Vc1}}{\mathrm{L1}}(1-\mathrm{D});\ \Delta iL_2=\frac{\mathrm{Vc1}}{\mathrm{L2}}-\frac{\mathrm{Vout}}{\mathrm{L2}}(1-\mathrm{D}) \quad (26) \quad \Delta \mathrm{V}_{c1}=\frac{\mathrm{IL1}}{\mathrm{C1}}(1-D)-\frac{\mathrm{IL2}}{\mathrm{C1}};\ \Delta \mathrm{V}_{out}=\frac{\mathrm{IL2}}{\mathrm{C2}}-\frac{\mathrm{Vout}}{\mathrm{Rc2}} \quad (27)$$

In steady state operation, the net inductor voltage should be zero.

In L_1:

$$\Delta iL_{1(ON)}+\Delta iL_{1(OFF)}=0 \tag{28}$$

$$\frac{\mathrm{Vin}}{\mathrm{L1}}DT+\frac{\mathrm{Vin}}{\mathrm{L1}}(1-\mathrm{D})\mathrm{T}-\frac{\mathrm{Vc1}}{\mathrm{L1}}(1-D)=0 \tag{29}$$

$$\frac{\mathrm{Vin}}{\mathrm{L1}}T=\frac{\mathrm{Vc1}}{\mathrm{L1}}(1-D)T \tag{30}$$

(30)

$$\mathbf{V_{c1}}=\frac{\mathbf{Vin}}{(\mathbf{1-D})} \tag{31}$$

In L_2:

$$\Delta i_{L2(ON)}+\Delta i_{L2(OFF)}=0 \tag{32}$$

$$V_{c1}D+V_{c1}(1-D)-V_{c1}D=V_{out}(1-D) \tag{33}$$

$$V_{c1}=V_{out}(1-D) \text{ and } \frac{\mathrm{Vin}}{(1-\mathrm{D})}=\mathrm{V}_{out}(1-\mathrm{D})^2 \tag{34}$$

$$\boldsymbol{V_{out}}=\frac{\mathbf{V_{in}}}{(\mathbf{1-D})^2} \tag{35}$$

The average current passing through the capacitor is zero:

$$i_{c(ON)}+i_{c(OFF)}=0 \tag{36}$$

$$-\frac{\mathrm{i_{L1}}}{\mathrm{C1}}(DT)+\frac{\mathrm{i_{L1}}}{\mathrm{C1}}(1-D)T-\frac{\mathrm{i_{L2}}}{\mathrm{C1}}(1-D)T=0 \tag{37}$$

$$-i_{L2}D+i_{L1}-i_{L1}D-i_{L2}+i_{L2}D=0 \tag{38}$$

$$i_{L1}(1-D)=i_{L2} \tag{39}$$

$$\mathbf{i_{L1}}=\frac{\boldsymbol{i_{L2}}}{(\mathbf{1-D})} \tag{40}$$

$$\mathrm{i_{L1}}=\frac{\mathrm{Io}}{(1-\mathrm{D})2} \tag{41}$$

$= \frac{(Vout)^2}{R} = \frac{V_S^2}{(1-D)^4 R}$ (42)

$\mathbf{L_1} = \frac{V_{out}(1-D)^2 . D}{\Delta IL1\ f}$ (43)

$\mathbf{L_2} = \frac{V_o(1-D)D}{\Delta I_{L2}\ f}$ (44)

In steady state operation of a capacitor, the net capacitor current must be zero during the switching period:

$$-\frac{Io}{C2}DT + \frac{ic2}{C2}(1-D) - (1-D)\frac{Io}{C2} = 0 \quad (45)$$

$-I_0D + i_{C2}(1-D) - I_0(1-D) = 0$ (46)

$-I_0D - I_0 + I_0D + IL_2(1-D) = 0$ (47)

$$\mathbf{I_{L2}} = \frac{Io}{(1-D)} \quad (48)$$

$|AQ| = DT * iL_2$ (49)

$C_1\Delta V_{c1} = DTiL_2$ (50)

$$V_{c1} = \frac{DT\ iL2}{C1} \quad (51)$$

$$iL_2 = \frac{Io}{(1-D)} \quad (52)$$

$$V_{c1} = \frac{\Delta T\frac{Io}{(1-D)}}{C1} \quad (53)$$

$$\mathbf{C_1} = \frac{D\ Io}{f\ (1-D)\Delta Vc1} \quad (54)$$

$|AQ| = DT * I_0$ (55)

$C_2\Delta V_{c2} = DTI_0$ (56)

$$\Delta V_{c2} = \frac{DTIo}{C2} \quad (57)$$

L1+L2 in terms of V_{in}:

$$L_1 = \frac{Vo\ D(1-D)}{\Delta I_{L1}\ f} \quad (58)$$

$$L_1 = \frac{Vin\ D}{\Delta I_{L1}\ f} \quad (59)$$

$L_2 = \frac{Vo\ D(1-D)}{\Delta I_{L2}\ f}$ (60)

$L_2 = \frac{\frac{Vin}{(1-D)^2}(1-D)D}{\Delta I_{L2}\ f}$ (61)

$L_2 = \frac{Vin\ D}{(1-D)\Delta I_{L2}\ f}$ (62)

Calculation:

$$L1 = \frac{Vo\ (1-D)^2 .\ D}{\Delta I_{L1} .\ f} = \frac{V_{in} .\ D}{\Delta I_{L1} .\ f} \quad (63)$$

$$L2 = \frac{Vo\ (1-D) .\ D}{\Delta I_{L2} .\ f} = \frac{V_{in} .\ D}{\Delta IL_2 .\ f} \quad (64)$$

$$I_{L1\ (avg.)} = \frac{Io}{(1-D)2} = \mathbf{5.136\ A} \quad (65)$$

$$I_{L2\ (avg.)} = \frac{Io}{1-D} = \mathbf{2.311\ A} \quad (66)$$

$$\Delta I_{L1} = 20\% \text{ of } I_{L1} = \mathbf{1.0272\ A} \quad (67)$$

$$\Delta I_{L2} = 20\% \text{ of } I_{L2} = \mathbf{0.4622\ A} \quad (68)$$

$V_{C1} = \frac{Vin}{1-D} = \mathbf{26.67\ V}$ (69)

$\Delta V_{C1} = 2\%$ of V_{C1} = **0.5334 A** (70)

$V_o = V_{C0}$ = **48 V** (71)

$\Delta V_{C0} = 2\%$ of V_{C0} = **0.96 V** (72)

$$C_1 = \frac{I_O \,.\, D}{f \,.\, (1-D) \,.\, \Delta VC1} \quad (73)$$

$$C_0 = \frac{I_O \,.\, D}{f \,.\, \Delta VC1} \quad (74)$$

$$R = {}^{V_0}/_{I_0} = \mathbf{46.154}\ \square \quad (75)$$

Table 1: *Specifications of components to be implemented further in circuit in Fig. 4.0*

Parameters	Values
INPUT VOLTAGE	12V
OUTPUT VOLTAGE	48 V
I_{in}	4.16 A
I_{out}	1.04 A
POWER RATING	50 W
L_1	72.115 µH
L_2	144.02 µH
C_1	86.7 µF
C_0	21.69 µF
R	46.154 □
f	50 kHz

4. Results and discussion

The hardware results have been determined from the oscilloscope along with supply of gate pulse through driver circuit.

4.2. Hardware Results

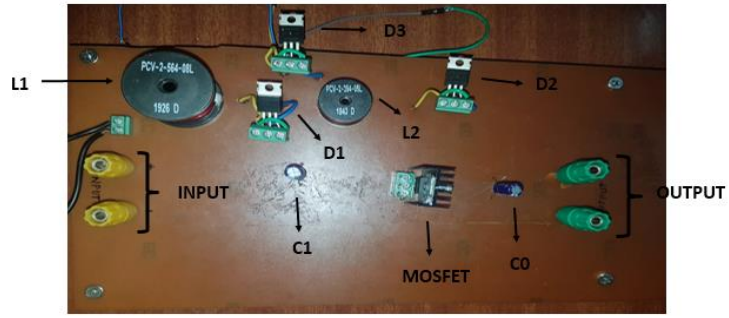

Fig 3. *Hardware apparatus*

- 12V is supplied as an input through the RPS.
- The input side inductor L1 rating 564uH, 8A stores the energy and the charges the capacitor C1 rating 41uF, 100V as Schottky diode D1 and D2 is forward biased while diode D3 is reversed biased during first cycle when the MOSFET IRF540 as switch is ON.
- During the next cycle diode D3 is forward biased while the diode D1 and D2 is reversed biased. The inductor L2 rating 390uH,5A is charged, and finally the capacitor stored energy and the inductor energy is released and stored in output capacitor C0 rating 41uF,100V and finally the desired output 48V is obtained at the output terminal.

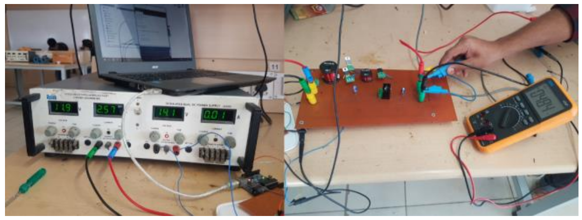

Fig 4. *Real-time testing of converter with driver circuit*

OUTPUTS FROM THE OSCILLOSCOPE

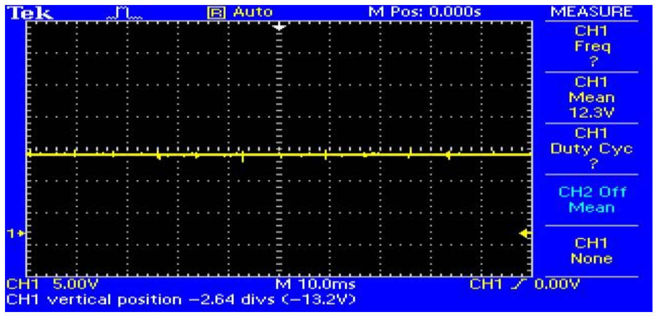

Fig 5. *Open loop Input voltage from voltage regulator (Vi = 12.3 V)*

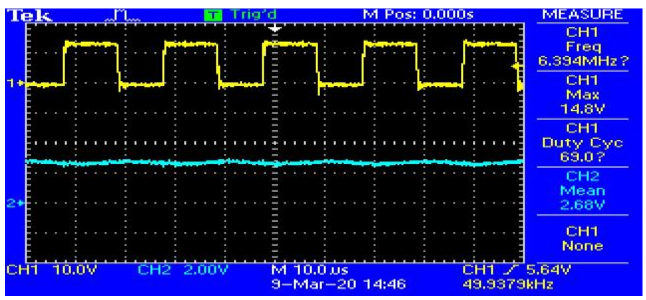

Fig 6. *Open loop Inductor L1 current*

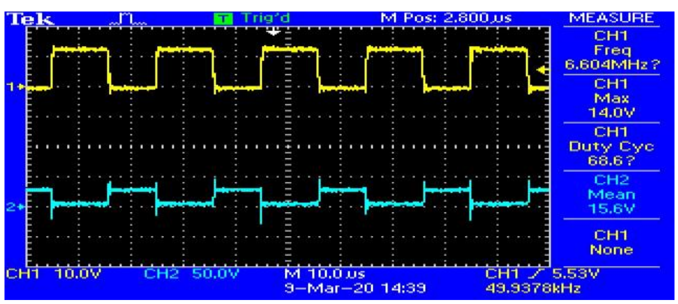

Fig 7. *Open loop Diode D1 voltage stress*
(V_{D1} = 15.6 V)

Parameter	**CALCULATED RESULTS**	**MEASURED RESULTS**
Voltage at input side	12 V	12.3 V

Voltage at output side	48 V	48.5 V
Duty Cycle	55%	51%
I_{in}	4.16 A	2.57 A
I_{out}	1.04 A	0.49 A
POWER RATING	50 W	31.611 W
L_1	72.115 µH	564 µH
L_2	144.02 µH	390 µH
C_1	86.7 µF	100 µF
C_0	21.69 µF	100 µF
R	46.154 □	48 □
f	50 kHz	49.9 kHz

Table 2: *Comparison between the hardware results and simulation results obtained by implementing similar constraints in both cases*

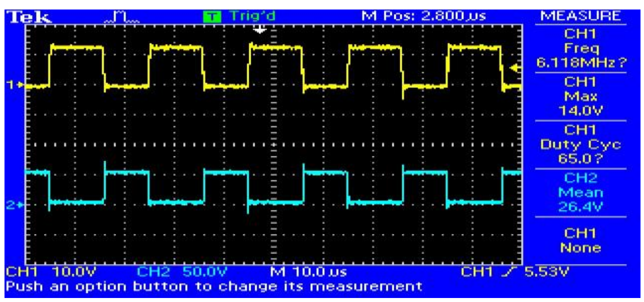

Fig 8. *Open loop Diode D3 voltage stress (V_{D3} = 26.4 V)*

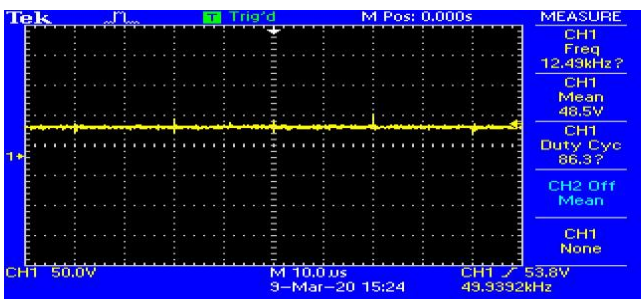

Fig 9.*Open loop output voltage (V_o = 48.5 V)*

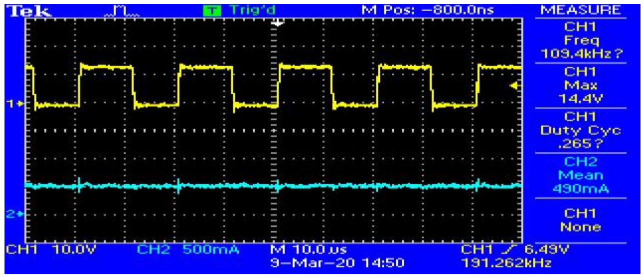

Fig 10.*Open loop output current (I_o = 490 mA)*

4.3 Comparison

It is observed that the input supplied is approximately 12 V in both cases of hardware and software. The Power rating of the device is 50 W on the books but due to some losses in the hardware implementation, it has come down to approximately 32 W. The output voltage has increased a fourfold to 48 V in both the simulation and hardware implementation which is exactly double of what is supposed to be achieved by a conventional boost converter i.e., 24 V. This is the effect of one switching parameter and thus, the doubling of the gain. Switching frequency was set at 50 kHz in both cases, which is supposed to be ideal in case of boost converters with high efficiency and high gain. With the above comparison, it is inferred that a proper functioning high efficiency Quadratic boost converter has been designed and implemented and therefore the results have been obtained by proper selection of constraints of the various components and conditions.

5. Conclusion

The theoretical analysis and the derivation of the QBC is presented in this paper. The simulation results are satisfactory. The functioning of the model is having considerable high efficiency due to one switch in operation at very high switching frequency. Hence simulation of the robust and effective model approves its implementation for residential or off-grid sector.

REFERENCES

1. Pranshu Agarwal and Rajeev Kumar Singh. 2014. A Modular Magnetically Coupled Quadratic Boost Converter for Micro-Source Applications. 7th IET International Conference on Power Electronics, Machines and Drives.
2. Surya Prabha V and M Ramaprasath.2018. Mathematical modelling and Performance analysis of Quadratic Boost Converter. International Journal of Scientific & Engineering Research. 9(3): 190-196.
3. Neng Zhang1, Danny Sutanto, Kashem M. Muttaqi, Bo Zhang and Dongyuan Qiu. High-voltage-gain quadratic boost converter with voltage multiplier. Institute of Engineering and Technology journals. ISSN 1755-4535, DOI:10.1049/iet-pel.2014.0767.
4. Wentao Jiang, Satyajit Hemant Chincholkar and Chok-You Chan. Modified voltage-mode controller for the quadratic boost converter with improved output performance. Institute of Engineering and Technology journals, ISSN 1755-4535, DOI: 10.1049/iet-pel.2018.5037.
5. K.H. Beena and Anish Benny. 2015. Analysis and Implementation of Quadratic Boost Converter for Nano-grid Applications. IJAREEIE. 4(7). 6043-6048.
6. Mustafa A. Al-Saffar, Esam H. Ismail, and Ahmad J. Sabzali. High Efficiency Quadratic Boost Converter. https://doi.org/10.1109/APEC.2012.6165978, ISSN - 1048-2334
7. S. Park and S. Choi. 2010. Soft-switched CCM boost converters with high voltage gain for high-power applications. IEEE Trans. Power Electron. 25(5). 1211–1216.
8. Jorge Alberto Morales-Saldana, Rodrigo Loera-palolo, E. Palacios Hernandez and Jorge Luis Gonzalez-Martinez. 2014. Modelling and control of a DC - DC quadratic boost converter with R2P2. IET Power Electron. 7(1). 11-22.
9. Hsieh Y, Chen J, Liang T and Yang L. 2013. Novel High step-up DC–DC converter for distributed generation system. IEEE Trans Ind Electron. 60(4):1473–1482.
10. S. Ozdemir, N. Altin, and I. Sefa. 2017. Fuzzy logic based MPPT controller for high conversion ratio quadratic boost converter. Int. J. Hydrogen Energy. 42(28). 17748–17759.
11. V. J. Samuel, G. Keerthi, and P. Mahalingam. 2020 Interleaved quadratic boost DC–DC converter with high voltage gain capability. Electr. Eng. 102(2), 651–662.

12. L. Xie, Z. Liu, and B. Zhang. 2020. A Modeling and Analysis Method for CCM Fractional Order Buck-Boost Converter by Using R–L Fractional Definition. J. Electr. Eng. Technol.15(4), 1651–1661.
13. P. M. García–Vite, C. A. Soriano–Rangel, J. C. Rosas–Caro, and F. Mancilla–David. 2017. A DC–DC converter with quadratic gain and input current ripple cancelation at a selectable duty cycle. Renew. Energy. 101. 431–436.
14. Y. Li and S. Sathiakumar. 2018. Quadratic DC-DC Boost Converter Using Coupled Inductors for High Step-Up Ratio. AMS 2017 - Asia Model. Symp. 2017 11th Int. Conf. Math. Model. Comput. Simul., no. 2. 133–138.
15. S. Balci, N. Altin, H. Komurcugil, and I. Sefa. 2019. Performance analysis of interleaved quadratic boost converter with coupled inductor for fuel cell applications. IECON Proc. (Industrial Electron. Conf. 3541–3546.
16. N. Altin. 2018. The Type-2 Fuzzy Logic Controller-Based Maximum Power Point Tracking Algorithm and the Quadratic Boost Converter for Pv System. *J. Electron. Mater.* 47(8). 4475–4485.
17. N. Zhang, G. Zhang, K. W. See, and B. Zhang. 2018. A single-switch quadratic buck-boost converter with continuous input port current and continuous output port current. IEEE Trans. Power Electron. 33(5). 4157–4166.
18. S. Belhimer, M. Haddadi, and A. Mellit. 2019. Design of a quadratic boost converter for a standalone PV system based on INC MPPT algorithm. Lect. Notes Electr. Eng., 519. 447–453.
19. R. Tiwari, K. Kumar, R. B. Neelakandan, S. Padmanaban, and P. W. Wheeler. 2018. Neural network based maximum power point tracking control with quadratic boost converter for PMSG—wind energy conversion system. Electron. 7(2).
20. S. Hasanpour, A. Mostaan, A. Baghramian, and H. Mojallali. 2019. Analysis, modeling, and implementation of a new transformerless semi-quadratic Buck–boost DC/DC converter. Int. J. Circuit Theory Appl. 47(6), 862–883.
21. S. W. Lee and H. L. Do. 2019. Quadratic Boost DC-DC Converter with High Voltage Gain and Reduced Voltage Stresses. IEEE Trans. Power Electron. 34(3). 2397–2404.
22. K. Patidar and A. C. Umarikar.2015. High step-up converters based on quadratic boost converter for micro-inverter. Electr. Power Syst. Res., 119.. 168–177.
23. J. Divya Navamani, K. Vijayakumar, and R. Jegatheesan. 2018. Non-isolated high gain DC-DC converter by quadratic boost converter and voltage multiplier cell. Ain Shams Eng. J. 9(4). 1397–1406.
24. P. Yang, J. Xu, G. Zhou, and S. Zhang. 2012. A new quadratic boost converter with high voltage step-up ratio and reduced voltage stress. Conf. Proc. - 2012 IEEE 7th Int. Power Electron. Motion Control Conf. - ECCE Asia, IPEMC 2012. 2. 1164–1168.
25. Kumar, N. Gupta, and V. Gupta. 2017. A Comprehensive Review on Grid-Tied Solar Photovoltaic System. J. Green Eng.7(1). 213–254.
26. F. Wang. 2018. A novel quadratic Boost converter with low current and voltage stress on power switch for fuel-cell system applications. Renew. Energy. 115. 836–845.